UNCERTAINTY OF ACCELERATION OF A PREMIXED LAMINAR UNSTABLE HYDROGEN FLAME

Elyanov, A.E.[1], Gavrikov, A.I.[1,2], Golub, V.V.[1], Kositsyn, I.V.[1,3], Mikushkin, A.Yu.[1,3] and Volodin, V.V.[1]

[1] Physical Gasdynamics Laboratory, Joint Institute for High Temperatures of the Russian Academy of Sciences, Izhorskaya st. 13 bld. 2, Moscow, 125412, Russia, elyanov14@physics.msu.ru

[2] Laboratory for Numerical Simulation of Complex Systems, NRC "Kurchatov Institute", Akademika Kurchatova pl., 1, Moscow, 123182, Russia, gavrikovandrey@yandex.ru

[3] Bauman Moscow State Technical University, ul. Baumanskaya 2-ya, 5/1, Moscow, 105005, Russia, lolipoenka@gmail.com

ABSTRACT

Unstable hydrogen-air flame behavior randomities are important for industrial safety, hydrogen infrastructure safety and nuclear power plant hydrogen safety problems. The paper is devoted to an experimental and theoretical study of the uncertainty in the acceleration of a premixed laminar unstable hydrogen flame. The results of experiments on spherical flame propagation in hydrogen-air mixtures with a hydrogen content of 10 to 60% are presented. The experiments were repeated up to 30 times in the same mixtures. A statistical analysis of the experimental results has been carried out. The scatter of the experimental data depending on the hydrogen content in the mixture was estimated. It was found to be between 8 to 17% for different mixtures with the same flame radius and mixture composition. Similar results were obtained using the numerical integration of the Sivashinsky equation of flame propagation.

1.0 INTRODUCTION

The formation of explosive combustion modes in stationary hydrogen-air mixtures often begins with slow laminar combustion [1]. The initial flame acceleration occurs when the smooth front is curved and its surface increases due to various instability mechanisms, of which the main ones are diffusive-thermal and hydrodynamic (Darrieus-Landau). Like all unstable processes, the flame acceleration front allows a certain scatter of parameters depending on the nature of the disturbances in the medium through which it propagates.

Previously, the authors showed that experimental data on the dynamics of the flame front for a hydrogen-air mixture with a hydrogen content of 15% under constant conditions can change from experiment to experiment [2,3]. The problem of differences in experimental data on flame acceleration in channels, the rate of spherical flame propagation and the rate of laminar combustion in gas mixtures obtained by different researchers have been raised more than once in the literature [4-6]. For the case of turbulent combustion, statistical models have been created that describe the scatter of combustion parameters [7,8]. Recently, more and more researchers are inclined to a probabilistic description of not only turbulent combustion modes, but also the processes of ignition [9] and propagation of unstable laminar flames [10]. In paper [10], the authors carried out a series of experiments on ignition and investigation of the initial stable stage of flame propagation in mixtures of hydrogen, ethylene, and propane with air and obtained a velocity spread.

One of the methods for the numerical and analytical description of the propagation velocity and the shape of the front of an exothermic reaction is the Sivashinsky integro-differential equation [11]. The equation describes the evolution of the surface corresponding to the front of a chemical reaction, the thickness of which is assumed to be infinitely small in comparison with the characteristic dimensions of the inhomogeneities. Originally formulated for a weakly nonlinear plane flame front, the equation

was adapted to describe an expanding flame [12] and a highly nonlinear flame that is thermodiffusively unstable [13].

The construction of the dynamics of propagation of the flame front by numerically solving the Sivashinsky equation was first carried out by D. Michelson and G. Sivashinsky in a flat two-dimensional formulation [14]. Subsequently, the Sivashinsky equation was solved in a two-dimensional formulation for an expanding flame numerically [15] and analytically [16]. In paper [17], the equation was supplemented with a complicated model of the chemical kinetics of the process. The paper [18] is devoted to the analysis of the dependence of the flame folding factor on time and the concentration of hydrogen in a hydrogen-air mixture using the numerical integration of the Sivashinsky equation in a flat two-dimensional formulation with a flame front length of about 2 m. The folding factor (or wrinkling factor) A/A_0 is called the ratio of the surface area of a folded unstable flame front to the area of a similar smoothed surface.

The initial distribution of disturbances in the paper [18] was modeled by "white noise" with average amplitude of 10^{-7} m. The results demonstrate for all mixtures a characteristic type of dependence of the folding coefficient on time for all mixtures: at the initial moment of time and during a specific induction period, the folding coefficient differs little from unity; then, in a short time, it increases to values 1.3–1.4; after that, fluctuations begin within 10% of the value with a general tendency to increase. It is also shown in the paper [18] that a decrease in the amplitude of the initial perturbations leads to an increase in the induction period. Other configurations of initial perturbations were not considered in this paper.

This article represents the results of an experimental and numerical study of the spread of velocities of the laminar unstable flame front. A series of time dependencies of the average flame front radius was obtained experimentally. Flame perturbations were obtained naturally from the instability of the igniting discharge and fluctuations in the parameters of the mixture. The dependencies of the average radius of the flame on time are obtained numerically for various amplitudes of the initial disturbances of the front.

2.0 INVESTIGATION METHODS

2.1 Experimental Setup

The experimental setup for the study of hydrogen combustion includes 2 main parts: a system for mixing gases and filling the shells and a system for visualizing and initiating combustion.

The gas section consists of a pressure gauge with 300 divisions, graduated per unit and a maximum pressure of 500 kPa. Thus, the error is 800 Pa. The combustible mixture was prepared in a cylinder (1) with a volume of 40 dm^3 at a maximum pressure of 500 kPa excess. The procedure for preparing the mixture is as follows. The cylinder was preliminarily evacuated to the limiting value of the vacuum pump – 1.1 Pa, then the cylinder was filled with air to atmospheric pressure by connecting to the atmosphere. After that, according to the same manometer, the cylinder was filled with hydrogen to a pressure corresponding to that required for studying the percentage mixture. In the end, air flowed into the cylinder from a compressor with a maximum pressure of 800 kPa. The mixture container was allowed to stand for at least 24 hours before using the mixture.

Visualization was carried out with an IAB-451 shadow device (2) with registration with a Phantom VEO 710S high-speed video camera (3). The main light source in the device was a xenon lamp (4). A transparent latex balloon (5) filled with gas from a cylinder through a gas main was placed between two optical parts of the IAB-451 instrument with a field of view with a diameter of 230 mm. The high-speed camera was shooting at speeds from 300 to 9000 frames per second, depending on the composition of the mixture, so that the number of frames of the spherical front was at least 10 pieces. The moment of the start of shooting was synchronized with the moment of initiation of combustion. The G5-63 pulse generator supplied a TTL signal with a voltage of 5 V to the camera and to the

commutator. The switch initiated a spark with an average energy of 50-100 mJ through the coil. The latex ball was pulled onto a special retaining fitting (6), the gas was fed through the line through the tee. In the upper part of the tee, a vacuum rubber gland is installed, in which a needle with an outer diameter of 1.5 mm is installed. An insulated guide is passed inside the needle. A spark is generated between the tip of the needle and the exposed part of the conductor with a gap of 1-3 mm.

The experiment's main parameters are as follows: atmospheric pressure, the pressure in the ball did not exceed the atmospheric pressure by 300 Pa. Room temperatures. Considering the air humidity in the compressor, the relative humidity of the mixture was less than 9%. The volume of the shells filled with a mixture with a hydrogen content of 10, 20, 50, and 60 vol.% was 4 dm^3, the radius of such shells was 10 cm. A mixture with a 30 vol.% hydrogen content was filled into shells with a volume of 0.5 dm^3 and a radius of 6 cm.

The critical flame radius in which buoyant forces will begin to play a substantial role is estimated by the following formula [19,20]:

$$\langle R\rangle_c = \frac{9}{4}\frac{{S_L}^2}{g}\frac{\Theta^3}{\Theta - 1},$$

where $\langle R\rangle$–mean radius of the flame front, S_L–laminar burning velocity, g - acceleration of gravity, $\Theta = \rho_u/\rho_b$–ratio of densities of the combustible mixture and combustion products. For mixtures with a hydrogen content of 20-60 vol. %, the value of $\langle R\rangle_c$ ranges from 70 cm to 10 m, this significantly exceeds the characteristic dimensions of the experiment. For mixture with a hydrogen content of 10 vol. % the value of $\langle R\rangle_c$ is 5 cm, i.e. at the late stages of flame propagation, the buoyancy of a cloud of combustion products plays a substantial role.

The images were subjected to automated processing by a program written in the MatLab environment. The obtained angular sweeps were converted into R-t diagrams, where each point was calculated by averaging the radii of all points on the front at each moment in time.

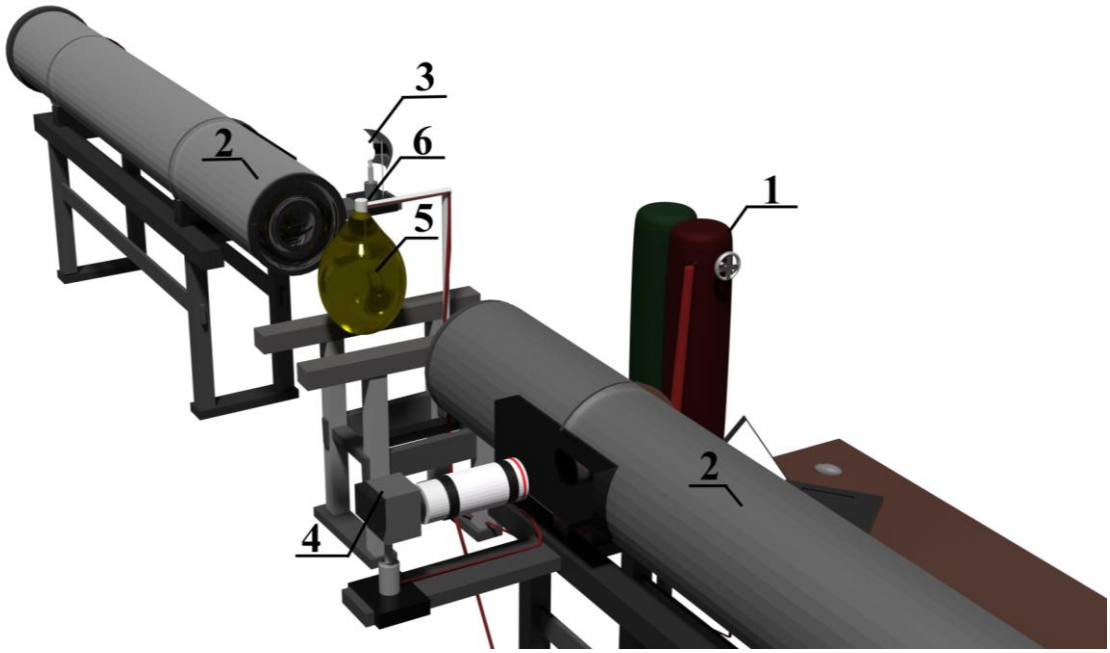

Figure 1. Experimental setup. 1 – gas cylinders, 2 – schlieren device, 3 – light source, 4 – high-speed camera, 5 – latex shell, 6 – fitting for gas injection and spark discharger.

2.2 Numerical Method

To determine the role of initial perturbations on the velocity of an unstable expanding globally spherical flame, we numerically integrated the evolutionary Sivashinsky equation for a two-dimensional expanding flame [12]:

$$\frac{\partial R}{\partial t} = \frac{\Theta S_L}{2\langle R\rangle^2}\left(\frac{\partial R}{\partial \varphi}\right)^2 + \frac{\delta S_L}{\langle R\rangle^2}\left(\frac{1}{2}Ze(1-Le)+1\right)\frac{\partial^2 R}{\partial \varphi^2} + \frac{(\Theta-1)S_L}{2\langle R\rangle}I(R) + \Theta S_L,$$

where $R(\varphi, t)$ – flame front radius at the angle of φ and in the time moment of t, δ–flame front thermal thickness, Ze–Zeldovich number, Le–Lewis number and the operator $I(R)$ is defined as:

$$I(R) = \frac{1}{\pi}\sum_{n=1}^{\infty} n \int_0^{2\pi} \cos[n(\varphi-\varphi^*)]\, R(\varphi^*)d\varphi^*.$$

For the numerical solution, the spatial and temporal variables were normalized to δ and δ/S_L, respectively. In accordance with the recommendations given in the paper [14], the step of the dimensionless spatial variable was maintained in the range from 1 to 2. At the initial moment of time, the flame front was set at points with a step along the angle $\Delta\varphi = 2\pi/2^N$, where $N \in \mathbb{N}$ and $1 < \Delta\varphi\langle R_0\rangle < 2$. With an increase in the average radius of the flame, when the step exceeded 2, the number of points along the angular coordinate doubled, and the radius values were interpolated from the values of neighboring points. The time step throughout the calculation was equal to 0.01 dimensionless time units.

The initial conditions were set as follows:

- the initial radius was 10 units (thickness of the flame front);
- three types of initial perturbations were added – random heights up to unity, harmonic with a frequency of 6 periods per circle, with an amplitude equal to one, and a single one with a length of 12 units and a height of 0.01.

Integration continued until reaching 300 units of dimensionless time, or from 1.98 to 682 ms, depending on the composition of the mixture.

3.0 RESULTS AND DISCUSSION

As a result of the experiments, frame-by-frame shadow images of the flame front were obtained (Figure Figure 2).

Using an automated processing program, the dependencies of the radius of the flame front on the angular coordinate were obtained. The point corresponding to the middle of the spark gap of the arrester was chosen as the center of the flame front. The average radius of the flame front was determined as the average value of the function $R(\varphi)$. An example of a set of R-t diagrams for 22 experiments in 10 vol.% and 24 experiments in 30 vol.% hydrogen mixtures is shown in Figure Figure 3. Figure 3 also shows R-t diagrams of spherical flame propagation in 30 vol.% hydrogen mixture from [21,22]. It can be seen that immediately after ignition, the flame speed is noticeably higher than in the experiments of the authors. This can be explained by the rather high ignition energy, the value of which is not indicated in these papers.

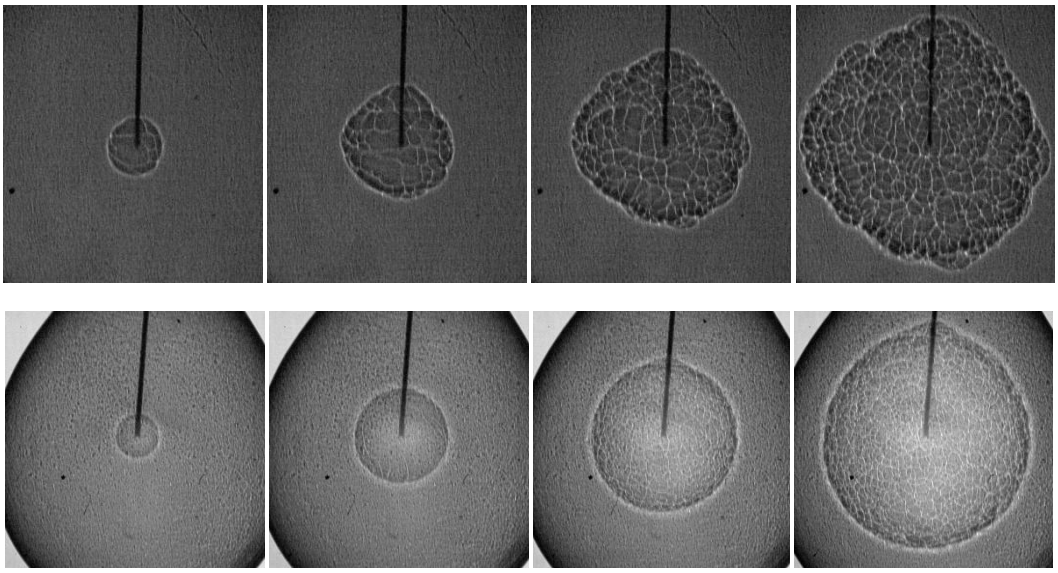

Figure 2. Shadow photographs of the flame front in a mixture with a hydrogen content of 10 vol.% at times 20, 40, 60, and 80 ms (top, from left to right) and 30 vol.% at times 0.83, 1.67, 2.5, and 3.33 ms (bottom, from left to right) after ignition. The photos are 127 mm wide.

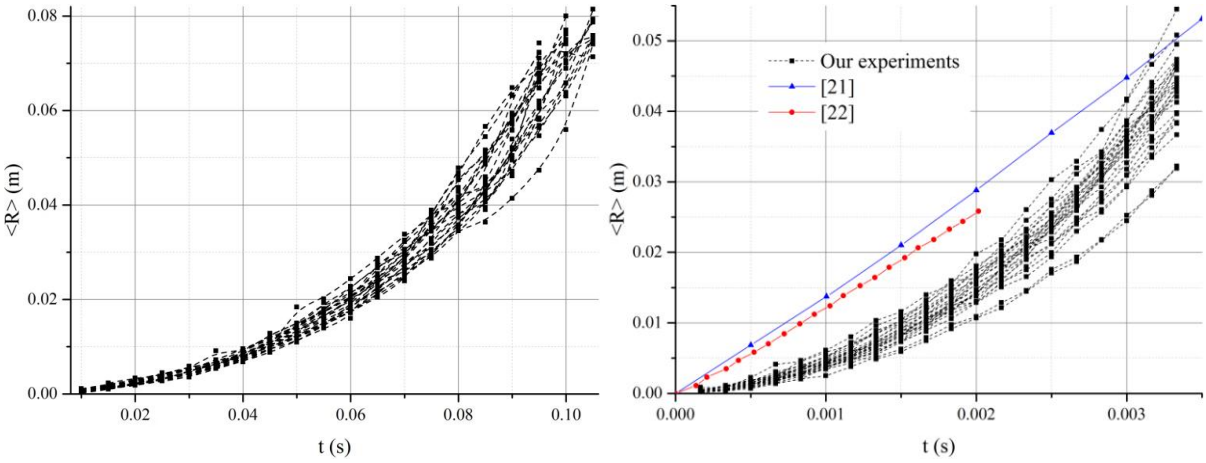

Figure 3. R-t diagrams for 22 experiments on spherical flame propagation in a hydrogen-air mixture with a hydrogen content of 10 vol.% (left) and 24 our experiments and experiments from [21,22] on spherical flame propagation in a hydrogen-air mixture with a hydrogen content of 30 vol.% (right).

When approximating R-t diagrams of flame front propagation by a power law:

$$\langle R\rangle = At^n, \qquad (1)$$

the exponent n is very different from the theoretically justified value of 1.33–1.5. This is since two stages of acceleration occur during the flame front propagation. Figure Figure 4 shows that the initial stage of propagation corresponds to the power of 1.15, the later stage corresponds to the power of 2.05. When the full R-t diagram is approximated by a power law, the constructed function takes into account this break, so the exponent becomes greater than 2. Within the framework of the problem proposed in the work, it is necessary to approximate the complete diagrams to obtain the values of the preexponential factor; therefore, the physical meaning of the degree n is omitted to simplify the analysis of the data scatters.

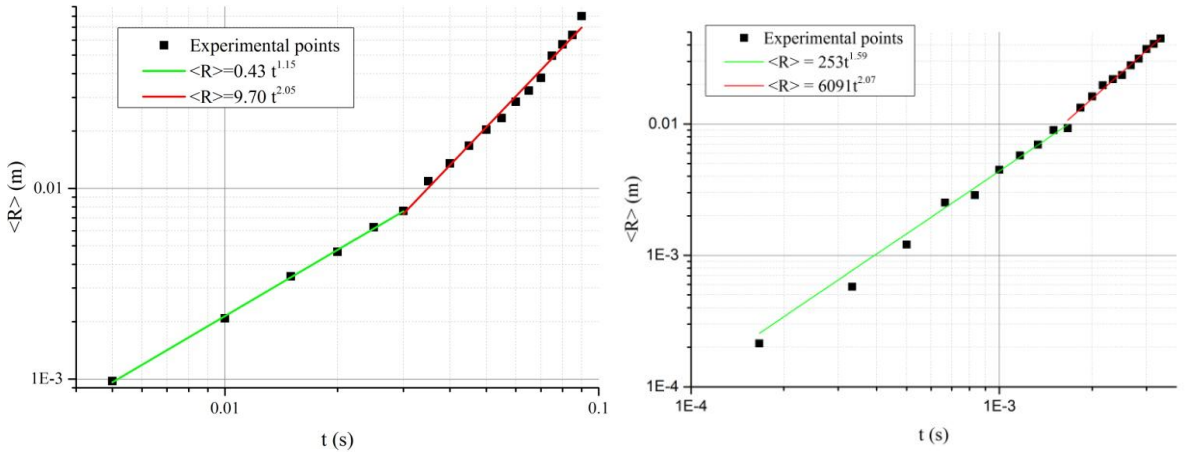

Figure 4. Examples of approximation of the R-t diagram of one experiment on spherical flame propagation in a hydrogen-air mixture with a hydrogen content of 10 vol.% (left) and 30 vol.% (right) using power-law dependences.

The experimental R-t diagrams were approximated by a power law (1). Then, within the framework of one composition of the gas mixture, the exponent n was averaged, and the R-t diagrams were again approximated by the power law (1), but with one mean value n. In this case, one value of the multiplier was obtained for each experiment. For each composition of the mixture, the dimension of the factor was the same. This made it possible to reduce the dependencies of the flame radius on time to a single parameter that allows comparison and statistical interpretation. Histograms and probability density functions of the preexponential factor of the power-law dependence of the average flame radius on time in mixtures with a hydrogen content of 10 to 60 vol.% are shown in Figure 5. Histograms and probability density functions of the preexponential factor of the power-law dependence of the average flame radius on time in mixtures with a hydrogen content of 10 to 60 vol.%.

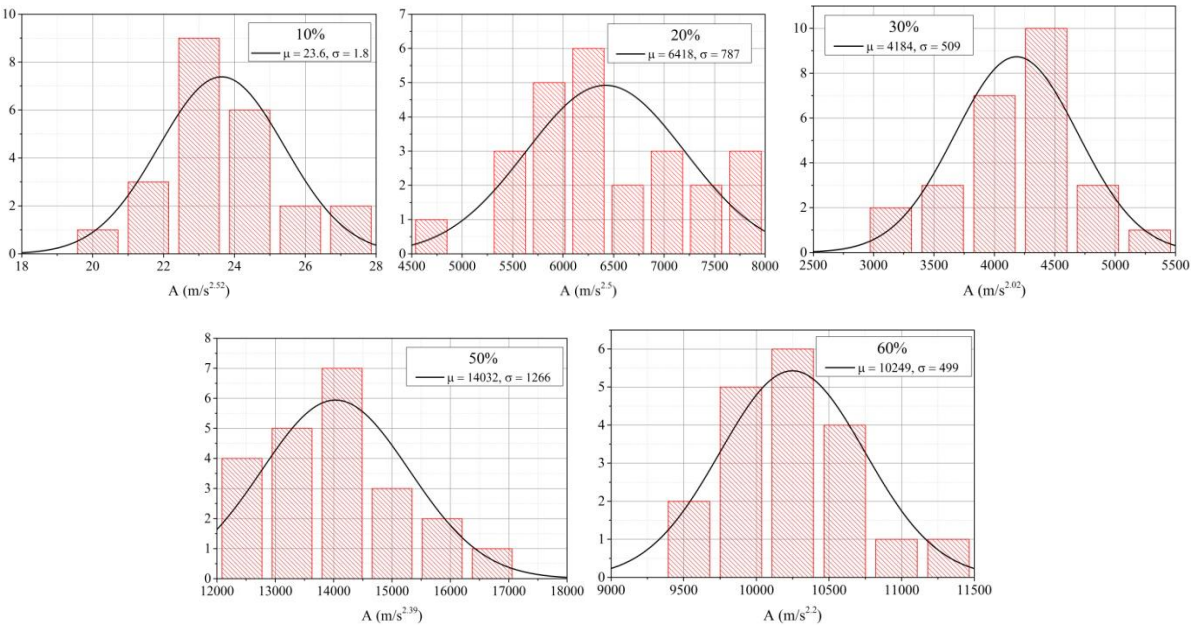

Figure 5. Histograms and probability density functions of the preexponential factor of the power-law dependence of the average flame radius on time in mixtures with a hydrogen content of 10 to 60 vol.%.

Analysis of the scatter of flame acceleration parameters requires setting different initial conditions. As a result of numerical simulation, the angular dependencies of the radius of the flame front at successive times (Figure 6) were obtained.

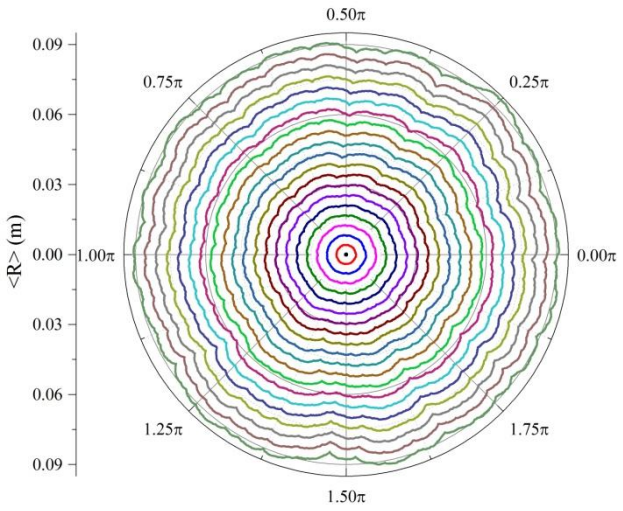

Figure 6. Calculated dependencies of the radius of the flame front on the angle at successive times. The interval between the graphs is 0.68 ms. A hydrogen-air mixture with a hydrogen content of 20 vol.%. Initial perturbations of random height up to a unit thickness of the flame front.

At each point in time, the average value of the radius was determined. From the obtained values, the dependencies of the average radius on time (Figure 7) were plotted. The calculated dependencies of the average radius of the flame front on time were approximated by dependencies of the form:

$$\langle R \rangle = At^{1.33} + R_0. \qquad (2)$$

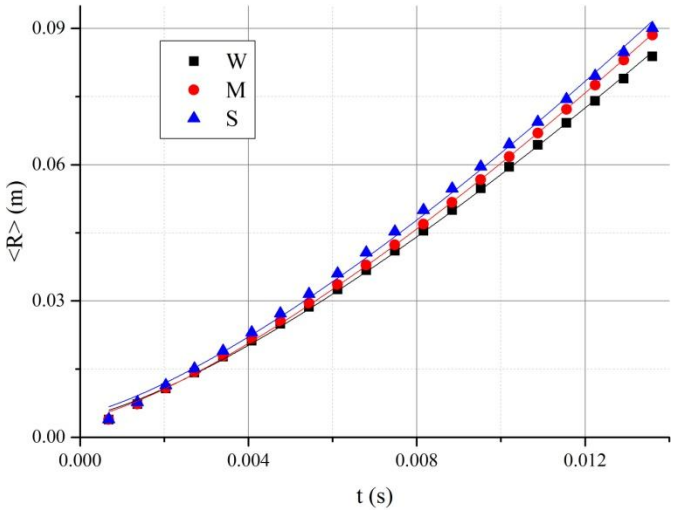

Figure 7. Calculated dependencies of the average radius of the flame front on time. A hydrogen-air mixture with a hydrogen content of 20 vol.%. Initial perturbations: random height up to one flame front thickness (S), harmonic with a frequency of 6 periods per circle and an amplitude equal to one (M), a single 12 units long, 0.01 high (W).

The parameters for approximating the results of numerical simulation are presented in Table 1. The spread of the values of the preexponential factor relative to the average is 3.8%.

Table 1. Parameters of approximation of the calculated R-t diagrams of flame propagation in a mixture with a hydrogen content of 15 vol.%.

Initial disturbances	A, m/s$^{1.33}$	R_0, m
single 12 units long, 0.01 high	24.40	$4.5*10^{-3}$
harmonic with a frequency of 6 periods per circle and an amplitude equal to one	25.74	$4.0*10^{-3}$
random height up to a unit thickness of the flame front	26.27	$5.1*10^{-3}$

Relative standard deviation (RSD) or coefficient of variation (CV) numerically equal to the ratio of the standard deviation to the mean as a percentage is a generally accepted numerical characteristic of the variation in data. The RSD obtained from the histograms of the distribution of the preexponential factor is shown in FigureFigure 8.

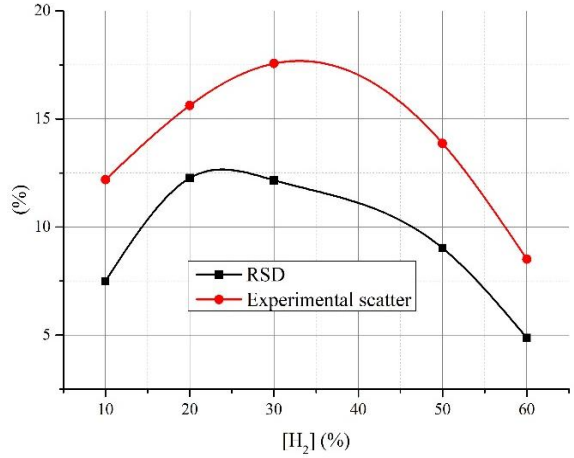

Figure 8. Dependencies of the relative experimental spread and the relative standard deviation of the preexponential factor A on the hydrogen content in the mixture.

One graph (Figure 8) plots the percentage between the average and maximum radius at the time when the average radius is close to 5 cm. It can be seen from the graph that the values obtained directly from the experimental data are higher than the relative standard deviation. This is directly due to the small amount of experimental data. In this work, each series of experiments consisted of 20–25 identical experiments. This amount may not be sufficient for a fair assessment of the spread of parameters. It is possible that there are no experiments with both high and low speed values. Thus, we assume that with an increase in the number of experiments, the scatter values will also increase. However, this assumption is unfounded for the RSD value. High repeatability of experiments can lead to both narrowing of the histogram and its expansion, which can affect the value of the standard deviation.

In this case, a few experiments do not interfere with judging the behavior of the scatter depending on the composition of the mixture. Over the entire range of hydrogen concentrations in the mixture, it can be seen that the maximum scatter is achieved in the region of the stoichiometric hydrogen concentration – 33 vol.%. A decrease in the instability of the flame front, characterized by an increase in the Lewis number with an increase in the fuel concentration in the mixture, should lead to the formation of a smooth flame surface. We assume that it is precisely the folded flame that is more subjected to the stochastic scatter of speeds. However, this pattern is not so clearly observed. On the other hand, an increase in the average front propagation speed when approaching the stoichiometric

hydrogen concentration can lead to a broadening of the data scatter. This is explained by the fact that the initial disturbances have time to develop to a greater extent and lead to their more significant influence on the front propagation. Mixtures with a hydrogen concentration higher than stoichiometric (50 and 60 vol.% hydrogen in the mixture) are less subject to scatter of values, since their surface becomes smooth.

The scatter values obtained using numerical simulation are noticeably lower than the experimental ones, which indicates the need to develop numerical methods for adequate modeling of the processes occurring in reality.

The RSD value can be taken into account in computer modeling of combustion propagation, analysis of destruction risks in case of accidents with a hydrogen scenario, as well as in the preparation and evaluation of experimental results. The natural character of the phenomenon makes it difficult to accurately simulate the combustion process, which must be taken into account when obtaining the calculation results.

4.0 CONCLUSIONS

A series of experiments on the combustion of hydrogen-air mixtures with 10, 20, 30, 50, and 60 vol.% hydrogen content in the mixture has been carried out.

The R-t diagrams of the flame front propagation are plotted. The values of the degree and pre-exponential factor were calculated for each series of experiments.

The RSD values were obtained and the scatter of the experimental data was estimated depending on the hydrogen content in the mixture.

Numerical integration of the Sivashinsky equation is carried out. With a change in the initial perturbations, a scatter of flame acceleration was obtained, similar to the experimental one.

The presented dependencies show the possibility of realizing various parameters with constant fuel concentration in the mixture and initial conditions.

ACKNOWLEDGEMENT

This research was funded by the RFBR, project number 20-31-70041.

REFERENCES

1. Bradley, D., Cresswell, T.M. and Puttock, J.S., Flame Acceleration due to Flame-Induced Instabilities in Large-Scale Explosions, *Combustion and Flame*, **124**, No. 4, 2001, pp. 551-559.
2. Elyanov, A.E., Golub, V.V., Korobov, A.E., Mikushkin, A.Yu., Petukhov, V.A. and Volodin, V.V., Lean Spherical Hydrogen–Air Flames at 4 Orders of Magnitude in Size and Ignition Energy, *Journal of Physics: Conference Series*, **1147**, 2019, p. 012047.
3. Volodin, V.V., Golub, V.V., Elyanov, A.E., Korobov, A.E., Mikushkin, A.Yu. and Petukhov, V.A., Effects of Hydrogen-Air Gas Mixture Volume and Initiation Type and Energy on the Propagation of a Spherical Flame Front, *Herald of the Bauman Moscow State Technical University, Series Natural Sciences*, **83**, No. 2, 2019, pp. 64-78.
4. Xu, C. and Konnov, A.A., Validation and Analysis of Detailed Kinetic Models for Ethylene Combustion, *Energy*, **43**, 2012, pp. 19-29.
5. Egolfopoulos, F.N., Hansen, N., Ju, Y., Kohse-Höinghaus, K., Law, C.K. and Qi, F., Advances and Challenges in Laminar Flame Experiments and Implications for Combustion Chemistry, *Progress in Energy and Combustion Science*, **43**, 2014, pp. 36-67.

6. Polezhaev, Yu.V. and Mostinsky, I.L., The Normal Flame Velocity and Analysis of the Effect of the System Parameters on This Velocity, *High Temperature*, 43, No. 6, 2005, pp. 937-946.
7. Thomas, G.O. and Oakley, G.L., On Practical Difficulties Encountered When Testing Flame and Detonation Arresters to BS 7244, *Transactions of the Institution of Chemical Engineers: Part B*, **71**, 1993, pp. 187-196.
8. Shepherd, J.E. and Lee, J.H.S., On the Transition from Deflagration to Detonation. Major Research Topics in Combustion. (Hussaini, M.Y., Kumar, A. and Voigt, F.G. Eds.), Springer-Verlag, New York, 1992, p. 439.
9. Bane, S.P.M., Ziegler, J.L., Boettcher, P.A., Coronel, S.A. and Shepherd, J.E., Experimental Investigation of Spark Ignition Energy in Kerosene, Hexane, and Hydrogen, *Journal of Loss Prevention in the Process Industries*, **26**, 2013, pp. 290-294.
10. Essmann, S., Markus, D., Grosshans, H. and Maas, U., Experimental Investigation of the Stochastic Early Flame Propagation After Ignition by a Low-Energy Electrical Discharge, *Combustion and Flame*, **211**, 2020, pp. 44-53.
11. Sivashinsky, G.I., Nonlinear Analysis of Hydrodynamic Instability in Laminar Flames – I. Derivation of Basic Equations, *Acta Astronautica*, **4**, 1977, pp. 1177-1206.
12. Filyand, L., Sivashinsky, G. and Frankel, M., On Self Acceleration of Outward Propagating Wrinkled Flames, *Physica D*, **72**, 1994, pp. 110-118.
13. Frankel, M. and Sivashinsky, G., On the Non-Linear Thermal Diffusive Theory of Curved Flames, *Journal of Physics*, **48**, 1987, pp. 25-28.
14. Michelson, D.M. and Sivashinsky, G.I., Nonlinear Analysis of Hydrodynamic Instability in Laminar Flames – II. Numerical Experiments, *Acta Astronautica*, **4**, 1977, pp. 1207-1221.
15. Michelson, D. and Sivashinsky, G., Thermal-Expansion Induced Cellular Flames, *Combustion and Flame*, **48**, 1982, pp. 211-217.
16. Minaev, S.S., Pirogov, E.A. and Sharypov, O.V., A Nonlinear Model for Hydrodynamic Instability of an Expanding Flame, *Combustion, Explosion, and Shock Waves*, **32**, No. 5, 1996, pp. 481-488.
17. Brailovsky, I., Gordon, P.V., Kagan, L. and Sivashinsky, G., Diffusive-Thermal Instabilities in Premixed Flames: Stepwise Ignition-Temperature Kinetics, *Combustion and Flame*, **162**, 2015, pp. 2077-2086.
18. Yanez, J. and Kuznetsov, M., An Analysis of Flame Instabilities for Hydrogen–Air Mixtures Based on Sivashinsky Equation, *Physics Letters A*, **380**, 2016, pp. 2549-2560.
19. Babkin, V., Vykhristuk, A.Y., Krivulin, V.N. and Kudriavcev, E., Convective Instability of Spherical Flames, *Archivum Combustionis*, **4**, No. 4, 1984, pp. 321-328. (in Russian)
20. Leblanc, L., Manoubi, M., Dennis, K., Liang, Z., and Radulescu, M.I., Dynamics of Unconfined Spherical Flames: Influence of Buoyancy, *Physics of Fluids*, **25**, 2013, p. 091106
21. Kim, W.-K., Mogi, T., and Dobashi, R., Fundamental Study on Accidental Explosion Behavior of Hydrogen-Air Mixtures in an Open Space, *International Journal of Hydrogen Energy*, **38**, 2013, pp. 8024-8029
22. Hu, E., Huang, Z., He, J., Jin, C., and Zheng, J., Experimental and Numerical Study on Laminar Burning Characteristics of Premixed Methane–Hydrogen–Air Flames, *International Journal of Hydrogen Energy*, **34**, 2009, pp. 4876-4888